A two-way molecular dialogue between embryo and endosperm is required for seed development

N. Doll, S. Royek, S. Fujita, S. Okuda, S. Chamot, A. Stintzi, Thomas Widiez, M. Hothorn, A. Schaller, N. Geldner, et al.

Title: A two-way molecular dialogue between embryo and endosperm required for seed development

Authors: N. M. Doll[1], S. Royek[2,†], S. Fujita[3,†,‡], S. Okuda[4,†], S. Chamot[1], A. Stintzi[2], T. Widiez[1], M. Hothorn[4], A. Schaller[2], N. Geldner[3], G. Ingram[1,*]

Affiliations:

[1]Laboratoire Reproduction et Développement des Plantes, University of Lyon, ENS de Lyon, UCB Lyon 1, CNRS, INRAE, F-69342, Lyon, France.

[2]Department of Plant Physiology and Biochemistry, University of Hohenheim, Stuttgart, Germany.

[3]Department of Plant Molecular Biology, University of Lausanne, 1015 Lausanne, Switzerland.

[4]Structural Plant Biology Laboratory, Department of Botany and Plant Biology, University of Geneva, 1211 Geneva, Switzerland.

*Correspondence to: gwyneth.ingram@ens-lyon.fr.

†equal contribution

‡current address: National Institute of Genetics, 1111 Yata, Mishima, Shizuoka 411-8540, Japan.

Abstract (129 words)**:** The plant embryonic cuticle is a hydrophobic barrier deposited *de novo* by the embryo during seed development. At germination it protects the seedling from water loss and is thus critical for survival. Embryonic cuticle formation is controlled by a signaling pathway involving the ABNORMAL LEAF SHAPE1 subtilase, and the two GASSHO receptor-like kinases. We show that a sulfated peptide, TWISTED SEED1 (TWS1), acts as a GASSHO ligand. Cuticle surveillance depends on the action of the subtilase which, unlike the TWS1 precursor and the GASSHO receptors, is not produced in the embryo but in the neighboring endosperm. Subtilase-mediated processing of the embryo-derived TWS1 precursor releases the active peptide, triggering GASSHO-dependent cuticle reinforcement in the embryo. A bidirectional molecular dialogue between embryo and endosperm thus safeguards cuticle integrity prior to germination.

One Sentence Summary: Compartmentalized proteolytic activation of a signal peptide provides spatial cues to ensure an intact embryo cuticle.

Main Text (2047 words): In Angiosperms, seeds comprise three genetically distinct compartments, the zygotic embryo and the endosperm, and the maternal seed coat. Their development must be tightly coordinated for seed viability. Here we have elucidated a bidirectional peptide-mediated signaling pathway between the embryo and the endosperm. This pathway regulates the deposition of the embryonic cuticle which forms an essential hydrophobic barrier separating the apoplasts of the embryo and endosperm. After germination, the cuticle - one of the critical innovations underlying the transition of plants from their original, aqueous environment to dry land - protects the seedling from catastrophic water loss (*1*, *2*).

Formation of the embryonic cuticle was previously shown to depend on two Receptor-Like Kinases (RLKs) GASSHO1/SCHENGEN3 (from here-on named GSO1) and GSO2, and on ALE1, a protease of the subtilase family (SBTs) (*2–5*). *gso1 gso2* and (to a lesser extent) *ale1* mutants produce a patchy, and highly permeable cuticle (*2*). Mutant embryos also adhere to surrounding tissues causing a seed-twisting phenotype (*6*). Since SBTs have been implicated in the processing of peptide hormone precursors (*7, 8, 9*), we hypothesized that ALE1 may be required for the biogenesis of the elusive inter-compartmental peptide signal required for GSO1/2-dependent cuticle deposition.

CASPARIAN STRIP INTEGRITY FACTORs (CIFs), a family of small sulfated signaling peptides, are ligands for GSO1 and GSO2 (*10–12*). CIF1 and CIF2 are involved in Casparian strip formation in the root endodermis (*10*, *11*). The function of CIF3 and CIF4 is still unknown. To assess the role of CIF peptides in cuticle development, the quadruple mutant (*cif1 cif2 cif3 cif4)* was generated (Fig. S1A). Neither cuticle permeability nor seed twisting phenotypes were

observed in this quadruple mutant (Fig. S1B-E). However, reduction (in the leaky *sgn2-1* allele (*10*)) or loss (in the *tpst-1* mutant (*13*)) of Tyrosyl-Protein Sulfotransferase (TPST) activity, results in seed-twisting and cuticle-permeability phenotypes resembling those observed in *ale1* mutants (Fig. 1A-D, Fig. S2 A-D). These data suggest that a sulfated peptide may act as the ligand of GSO1/2 during seed development.

Consistent with the hypothesis that TPST acts in the same pathway as GSO1 and GSO2, no difference was observed between the phenotype of *tpst-1 gso1-1 gso2-1* triple and *gso1-1 gso2-1* double mutants (Fig. S2E). In contrast, TPST and ALE1 appear to act synergistically, as a phenotype resembling that of *gso1 gso2* double mutants was observed in *tpst-1 ale1-4* double mutants (Fig. 1E-I) (Fig. S2F-J). This result supports the hypothesis that TPST and ALE1 act in parallel regarding their roles in embryonic cuticle formation, possibly through independent post-translational modifications contributing to the maturation of the hypothetical peptide signal.

Identification of the peptide signal was facilitated by a study of TWISTED SEED1 (TWS1) (*14*), that reported a loss-of-function phenotype strikingly similar to that of *gso1 gso2* double mutants. Because existing alleles of *TWS1* are in the WS background, we generated new CRISPR alleles (*tws1-3* to *tws1-10)* in the Col-0 background, and confirmed the phenotype of resulting mutants (Fig. 1, Fig. S3). No additivity was observed when loss-of-function alleles of *TWS1* and of other pathway components (*GSO1, GSO2, TPST* and *ALE1*) were combined, providing genetic evidence for *TWS1* acting in the GSO signaling pathway (Fig. S4). Furthermore, gaps in the cuticle of embryos and cotyledons similar to those observed in *ale1* and *gso1 gso2* mutants *(2),* were detected in both the *tws1* mutants and *tpst* mutants (Fig. 1 J-N, Fig. S5). Inspection of the TWS1 protein sequence revealed a region with limited similarity to CIF peptides including a DY motif which marks the N-terminus of the CIFs (Fig. 1O), and is the minimal motif required for tyrosine sulfation

by TPST (*15*). Corroborating the functional importance of the putative peptide domain, the *tws1-6* allele (deletion of six codons in the putative peptide-encoding region) and the *tws1-5* allele (substitution of eight amino acids including the DY motif) both showed total loss of function of the TWS1 protein (Fig. S3).

We tested whether TWS1 is a substrate of ALE1 by co-expression of ALE1:(His)6 and TWS1:GFP-(His)6 fusion proteins in tobacco (*N. benthamiana*) leaves. A specific TWS1 cleavage product was observed upon co-expression of ALE1 but not in the empty-vector control suggesting that TWS1 is processed by ALE1 *in planta* (Fig. 1P). Likewise, recombinant TWS1 expressed as GST-fusion in *E. coli* was cleaved by purified ALE1 *in vitro*. (Fig. 1Q). Mass spectroscopy analysis of the TWS1 cleavage product purified from tobacco leaves showed that ALE1 cleaves TWS1 between His_{54} and Gly_{55} (Fig. S6). These residues are important for cleavage site selection, as ALE1-dependent processing was not observed when either His_{54} or Gly_{55} was substituted by site-directed mutagenesis (Fig. 1Q). His_{54} corresponds to the C-terminal His or Asn of CIF peptides (Fig. 1O). The data thus suggest that ALE1-mediated processing of the TWS1 precursor marks the C-terminus of the TWS1 peptide. Because the CIF1 and CIF2 peptides are located at the very end of their respective precursors, C-terminal processing could represent a mechanism of peptide activation operating in the developing seed but not in the root. A summary of TWS1 modifications is provided in Fig. 1R.

To test the biological activity of TWS1, the predicted peptide encompassing the conserved N-terminal DY-motif and the C-terminus defined by the ALE1 cleavage site was custom-synthesized in tyrosine-sulfated form. As synthetic TWS1 cannot easily be applied to developing embryos, a root bioassay for CIF activity was used. In wild-type roots TWS1 induced ectopic endodermal lignification as previously observed for the CIF1 and CIF2 peptides (*12*). TWS1 activity was

GSO1-dependent, suggesting that processed TWS1 peptide can replace CIF1 and CIF2 as a ligand for GSO1 during Casparian strip formation (Fig. 2A) (Fig. S7). Supporting this, TWS1 application complemented the *cif1 cif2* mutant, albeit with reduced activity compared to CIF2 (Fig. 2B, Fig. S8). TWS1 activity in this assay was reduced when sulfation on the DY motif was missing (Fig. 2B). Versions of TWS1 in which Y_{33} was mutated to either F or T only partially complemented the mutant phenotype of *tws1-4* (Fig S9), consistent with a residual but weak activity for non-sulfated TWS1 *in vivo*, and with the weak loss-of-function phenotype of the *tpst-1* mutant.

To confirm TWS1 as a ligand of GSO1 and GSO2, the interaction of the synthetic peptide with the leucine-rich repeat (LRR) ectodomains of the receptors was analyzed in grating – coupled interferometry binding assays. GSO1 bound sulfated TWS1 with a K_D of ~ 30 nM (Fig. 2C). The observed binding affinity is ~10 fold lower compared to the CIF2 peptide (K_D = 2.5 nM) (Fig. S10), which is consistent with the reduced ability of TWS1 to complement the root phenotype of the *cif1 cif2* double mutant (Fig. 2B). Sulfated TWS1 also bound to the LRR domain of GSO2, albeit with slightly reduced affinity (K_D ~ 100 nM) (Fig.2D). As previously shown for other CIF peptides (*11*), tyrosine sulfation was critical for the interaction of TWS1 with GSO1 and GSO2 *in vitro* (Fig. 2E,F). Technical issues at high peptide concentrations may explain discrepancies between *in vitro* binding assays and the *in vivo* activity of non-sulfated TWS1. *In vivo* activities for non-sulfated versions of other normally-sulfated peptides, including CIF2, have been reported *(11,16-18)*. Adding a 3AA C-terminal extension to the sulfated TWS1 peptide reduced binding affinity to both GSO1 and GSO2 (Fig. S10), consistent with the need for ALE1-mediated C-terminal processing for efficient signaling.

Taken together, our results suggest the sulfated TWS peptide as the missing link in the inter-compartmental signaling pathway for embryonic cuticle formation. The activities of ALE1 and

TPST both contribute to the formation of the bioactive peptide (Fig. 1R) which is perceived by GSO1 and GSO2 to ensure appropriate cuticle deposition.

To understand how the elements of the signaling pathway cooperate to ensure the formation of a functional cuticle, we analyzed their spatial organization. *In silico* data indicate that the *TPST* gene is expressed in all seed tissues (Fig. S11) (*19, 20*). To investigate in which compartment TPST (which acts cell autonomously (*13*)) is required for TWS1 maturation, reciprocal crosses and complementation assays using tissue specific promoters were performed. No cuticle permeability defects were observed when homozygous mutants were pollinated with wild-type pollen, confirming their zygotic origin. (Fig. 3A-C). Expressing TPST under the ubiquitously active *RPS5A* promoter (*21*), or the *PIN1* promoter (which is embryo-specific in seed (Fig. S12)) complements *tpst-1* cuticle defects. In contrast no complementation was observed using the endosperm-specific *RGP3* promoter (*22*), indicating that TPST activity is required for TWS1 sulfation specifically in the embryo to ensure cuticle integrity (Fig. 3D) (Fig. S13). Consistent with this observation, and with a previous report (*14*), the *TWS1* promoter was found to drive expression specifically in the developing embryo from the early globular stage onwards (Fig. 3E) (Fig S14). The *TPST* promoter (*10*) drove expression throughout the embryo proper at the onset of embryo cuticle establishment (globular stage) before becoming restricted to the root tip (Fig. S11). We conclude that the TWS1 peptide is both sulfated and secreted specifically in the embryo.

However, production of mature TWS1 requires a C-terminal cleavage event that we have shown to be mediated by ALE1. *ALE1* is expressed only in the endosperm (*4, 23*), on the opposite side of the nascent cuticle to the GSO1 and GSO2 receptors, which are localized on the membranes of the epidermal cells that produce the cuticle (Fig. S15-17) *(2)*. Our data thus support a model in which activation of the GSO signaling pathway depends on the diffusion of the TWS1 peptide precursor

to the endosperm, where it is cleaved and activated by ALE1 before diffusing back to the embryo to trigger GSO1/2-dependent cuticle deposition. An intact cuticle would separate the subtilase from its substrate, terminating signaling.

Expressing *ALE1* in the embryo, under the control of the *TWS1* promoter, provided support for this model. Multiple transformants were obtained in *tws1* mutants, but not in the wild-type background. When *tws1* plants from 4 independent plants carrying the *pTWS1:ALE1* transgene were pollinated with wild-type pollen, introducing a functional *TWS1* allele into the zygotic compartments, and thus inducing colocalization of TWS1 precursors, ALE1, GSO1 and GSO2 in the embryo, premature embryo growth arrest was observed in all seeds. This leads to severe shriveling of all seeds at maturity (Fig. 3F-M) (Fig. S18, S19). A proportion of seeds could nonetheless germinate to give developmentally normal plants (Fig. S20) indicating that co-expression of all signaling components in the embryo, although detrimental to embryo development does not lead to a complete loss of viability. Growth arrest may be due to constitutive embryonic activation of the *GSO1/GSO2* signaling pathway, and indeed stress-responsive genes shown to require GSO1/GSO2 signaling for expression in the seed (*2*) were upregulated in seeds co-expressing GSO1, GSO2, TWS1 and ALE1 in the embryo (Fig. S21). We thus postulate that the spatial separation of the TWS1 precursor and the GSO receptors from the activating protease by cuticle is required for signaling attenuation.

We next tested if CIF1, CIF2 and TWS1 could complement *tws1* and *ale1* mutants when expressed in the endosperm (under the *RGP3* promoter). All three peptides complemented *tws1* mutants, confirming that retrograde peptide movement from endosperm to embryo is sufficient to allow integrity monitoring (Fig. 3N and Fig. S22). Lack of full complementation could reflect suboptimal N-terminal processing or sulfation in the endosperm. CIF1 and CIF2 (lacking C-terminal

extensions) complemented *ale1* mutants much more efficiently than TWS1 (Fig. S23). Weak complementation of *ale1* by TWS1 may reflect the presence of redundantly-acting subtilases in the endosperm, as suggested by the weak phenotype of *ale1* mutants.

The proposed bidirectional signaling model allows efficient embryo cuticle integrity monitoring. The sulfated TWS1 precursor is produced by the embryo and secreted (probably after N-terminal cleavage of the pro-peptide) to the embryo apoplast. In the absence of an intact cuticular barrier, it can diffuse to the endosperm and undergo activation by ALE1 (and potentially other subtilases). Activated TWS1 peptide then leaks back through cuticle gaps to bind the GSO1 and GSO2 receptors and activate local gap repair (Fig. 3O). When the cuticle is intact, proTWS1 peptides are confined to the embryo where they remain inactive.

Our results demonstrate a role for a subtilase in providing spatial specificity to a bidirectional peptide signaling pathway. In contrast, the related CIF1, CIF2 and GSO1-dependent signaling pathway controlling Casparian strip integrity is uni-directional, negating the need for C-terminal cleavage-mediated peptide activation (*10*, *12*). Both pathway components and their spatial organization differ between the two systems, suggesting an independent recruitment of the GSO receptors to different integrity monitoring functions within the plant.

References and Notes:

1. C. Delude, S. Moussu, J. Joubès, G. Ingram, F. Domergue, Plant Surface Lipids and Epidermis Development. Subcell. Biochem. 86, 287–313 (2016).

2. A. Creff, L. Brocard, J. Joubès, L. Taconnat, N. M. Doll, A.-C. Marsollier, S. Pascal, R. Galletti, S. Boeuf, S. Moussu, T. Widiez, F. Domergue, G. Ingram, A stress-response-related inter-compartmental signalling pathway regulates embryonic cuticle integrity in Arabidopsis. PLoS Genet. 15, e1007847 (2019).

3. R. Tsuwamoto, H. Fukuoka, Y. Takahata, GASSHO1 and GASSHO2 encoding a putative leucine-rich repeat transmembrane-type receptor kinase are essential for the normal development of the epidermal surface in Arabidopsis embryos. Plant J. Cell Mol. Biol. 54, 30–42 (2008).

4. H. Tanaka, H. Onouchi, M. Kondo, I. Hara-Nishimura, M. Nishimura, C. Machida, Y. Machida, A subtilisin-like serine protease is required for epidermal surface formation in Arabidopsis embryos and juvenile plants. Dev. Camb. Engl. 128, 4681–4689 (2001).

5. Q. Xing, A. Creff, A. Waters, H. Tanaka, J. Goodrich, G. C. Ingram, ZHOUPI controls embryonic cuticle formation via a signalling pathway involving the subtilisin protease ABNORMAL LEAF-SHAPE1 and the receptor kinases GASSHO1 and GASSHO2. Dev. Camb. Engl. 140, 770–779 (2013).

6. S. Moussu, N. M. Doll, S. Chamot, L. Brocard, A. Creff, C. Fourquin, T. Widiez, Z. L. Nimchuk, G. Ingram, ZHOUPI and KERBEROS Mediate Embryo/Endosperm Separation by Promoting the Formation of an Extracuticular Sheath at the Embryo Surface. Plant Cell. 29, 1642–1656 (2017).

7. A. Schaller, A. Stintzi, S. Rivas, I. Serrano, N. V. Chichkova, A. B. Vartapetian, D. Martínez, J. J. Guiamét, D. J. Sueldo, R. A. L. van der Hoorn, V. Ramírez, P. Vera, From structure to function - a family portrait of plant subtilases. New Phytol. 218, 901–915 (2018).

8. N. Stührwohldt, A. Schaller, Regulation of plant peptide hormones and growth factors by post-translational modification. Plant Biol. (Suppl 1), 49–63 (2019).

9. K. Schardon, M. Hohl, L. Graff, J. Pfannstiel, W. Schulze, A. Stintzi, A. Schaller, Precursor processing for plant peptide hormone maturation by subtilisin-like serine proteinases. Science. 354, 1594–1597 (2016).

10. V. G. Doblas, E. Smakowska-Luzan, S. Fujita, J. Alassimone, M. Barberon, M. Madalinski, Y. Belkhadir, N. Geldner, Root diffusion barrier control by a vasculature-derived peptide binding to the SGN3 receptor. Science. 355, 280–284 (2017).

11. S. Okuda, S. Fujita, A. Moretti, U. Hohmann, V. Gonzalez Doblas, Y. Ma, A. Pfister, B. Brandt, N. Geldner, M. Hothorn, Molecular mechanism for the recognition of sequence-divergent CIF peptides by the plant receptor kinases GSO1/SGN3 and GSO2. bioRxiv, 692228.

12. T. Nakayama, H. Shinohara, M. Tanaka, K. Baba, M. Ogawa-Ohnishi, Y. Matsubayashi, A peptide hormone required for Casparian strip diffusion barrier formation in Arabidopsis roots. Science. 355, 284–286 (2017).

13. R. Komori, Y. Amano, M. Ogawa-Ohnishi, Y. Matsubayashi, Identification of tyrosylprotein sulfotransferase in Arabidopsis. Proc. Natl. Acad. Sci. U. S. A. 106, 15067–15072 (2009).

14. E. Fiume, V. Guyon, C. Remoué, E. Magnani, M. Miquel, D. Grain, L. Lepiniec, TWS1, a Novel Small Protein, Regulates Various Aspects of Seed and Plant Development. Plant Physiol. 172, 1732–1745 (2016).

15. H. Hanai, D. Nakayama, H. Yang, Y. Matsubayashi, Y. Hirota, Y. Sakagami, Existence of a plant tyrosylprotein sulfotransferase: novel plant enzyme catalyzing tyrosine O-sulfation of preprophytosulfokine variants in vitro. FEBS Lett. 470, 97–101 (2000).

16. Y. Matsubayashi, Y. Sakagami, Characterization of specific binding sites for a mitogenic sulfated peptide, phytosulfokine-alpha, in the plasma-membrane fraction derived from Oryza sativa L. Eur. J. Biochem. 262, 666–671 (1999).

17. A. Kutschmar, G. Rzewuski, N. Stührwohldt, G. T. S. Beemster, D. Inzé, M. Sauter, PSK-α promotes root growth in Arabidopsis. New Phytol. 181, 820–831 (2009).

18. Y. Matsuzaki, M. Ogawa-Ohnishi, A. Mori, Y. Matsubayashi, Secreted peptide signals required for maintenance of root stem cell niche in Arabidopsis. Science. 329, 1065–1067 (2010).

19. B. H. Le, C. Cheng, A. Q. Bui, J. A. Wagmaister, K. F. Henry, J. Pelletier, L. Kwong, M. Belmonte, R. Kirkbride, S. Horvath, G. N. Drews, R. L. Fischer, J. K. Okamuro, J. J. Harada, R. B. Goldberg, Global analysis of gene activity during Arabidopsis seed development and identification of seed-specific transcription factors. Proc. Natl. Acad. Sci. U. S. A. 107, 8063–8070 (2010).

20. A. V. Klepikova, A. S. Kasianov, E. S. Gerasimov, M. D. Logacheva, A. A. Penin, A high resolution map of the Arabidopsis thaliana developmental transcriptome based on RNA-seq profiling. Plant J. Cell Mol. Biol. 88, 1058–1070 (2016).

21. D. Weijers, Franke-van Dijk, M., R. J. Vencken, Quint, A., Hooykaas, P., Offringa, R., An Arabidopsis Minute-like phenotype caused by a semi-dominant mutation in a RIBOSOMAL PROTEIN S5 gene. Dev. Camb. Engl. 128, 4289–4299 (2001).

22. G. Denay, A. Creff, S. Moussu, P. Wagnon, J. Thévenin, M.-F. Gérentes, P. Chambrier, B. Dubreucq, G. Ingram, Endosperm breakdown in Arabidopsis requires heterodimers of the basic helix-loop-helix proteins ZHOUPI and INDUCER OF CBP EXPRESSION 1. Dev. Camb. Engl. 141, 1222–1227 (2014).

23. S. Yang, N. Johnston, E. Talideh, S. Mitchell, C. Jeffree, J. Goodrich, G. Ingram, The endosperm-specific ZHOUPI gene of Arabidopsis thaliana regulates endosperm breakdown and embryonic epidermal development. Dev. Camb. Engl. 135, 3501–3509 (2008).

24. A. Pfister, M. Barberon, J. Alassimone, L. Kalmbach, Y. Lee, J. E. M. Vermeer, M. Yamazaki, G. Li, C. Maurel, J. Takano, T. Kamiya, D. E. Salt, D. Roppolo, N. Geldner, A receptor-like kinase mutant with absent endodermal diffusion barrier displays selective nutrient homeostasis defects. eLife. 3, e03115 (2014).

25. D. Roppolo, B. De Rybel, V. D. Tendon, A. Pfister, J. Alassimone, J. E. M. Vermeer, M. Yamazaki, Y.-D. Stierhof, T. Beeckman, N. Geldner, A novel protein family mediates Casparian strip formation in the endodermis. Nature. 473, 380–383 (2011).

26. J. Friml, A. Vieten, M. Sauer, D. Weijers, H. Schwarz, T. Hamann, R. Offringa, G. Jürgens, Efflux-dependent auxin gradients establish the apical–basal axis of Arabidopsis. Nature. 426, 147 (2003).

27. Z.-P. Wang, H.-L. Xing, L. Dong, H.-Y. Zhang, C.-Y. Han, X.-C. Wang, Q.-J. Chen, Egg cell-specific promoter-controlled CRISPR/Cas9 efficiently generates homozygous mutants for multiple target genes in Arabidopsis in a single generation. Genome Biol. 16, 144 (2015).

28. F. Fauser, S. Schiml, H. Puchta, Both CRISPR/Cas-based nucleases and nickases can be used efficiently for genome engineering in Arabidopsis thaliana. Plant J. 79, 348–359 (2014).

29. E. Logemann, R. P. Birkenbihl, B. Ülker, I. E. Somssich, An improved method for preparing Agrobacterium cells that simplifies the Arabidopsis transformation protocol. Plant Methods. 2, 16 (2006).

30. T. Tanaka, H. Tanaka, C. Machida, M. Watanabe, Y. Machida, A new method for rapid visualization of defects in leaf cuticle reveals five intrinsic patterns of surface defects in Arabidopsis. Plant J. 37, 139–146 (2004).

31. U. Roshan, D. R. Livesay, Probalign: multiple sequence alignment using partition function posterior probabilities. Bioinforma. Oxf. Engl. 22, 2715–2721 (2006).

32. D. Kurihara, Y. Mizuta, Y. Sato, T. Higashiyama, ClearSee: a rapid optical clearing reagent for whole-plant fluorescence imaging. Development. 142, 4168–4179 (2015).

33. R. Ursache, T. G. Andersen, P. Marhavý, N. Geldner, A protocol for combining fluorescent proteins with histological stains for diverse cell wall components. Plant J. 93, 399–412 (2018).

34. R Core Team, R: A language and environment for statistical computing. R Foundation for Statistical Computing, Vienna, Austria. (2013).

35. Y. Hashimoto, S. Zhang, G. W. Blissard, Ao38, a new cell line from eggs of the black witch moth, Ascalapha odorata (Lepidoptera: Noctuidae), is permissive for AcMNPV infection and produces high levels of recombinant proteins. BMC Biotechnol. 10, 50 (2010).

36. M. Fairhead, M. Howarth, Site-specific biotinylation of purified proteins using BirA. Methods Mol. Biol. Clifton NJ. 1266, 171–184 (2015).

37. A. P. Gleave, A versatile binary vector system with a T-DNA organisational structure conducive to efficient integration of cloned DNA into the plant genome. Plant Mol. Biol. 20, 1203–1207 (1992).

38. A. Shevchenko, M. Wilm, O. Vorm, M. Mann, Mass spectrometric sequencing of proteins silver-stained polyacrylamide gels. Anal. Chem. 68, 850–858 (1996).

39. J. V. Olsen, L. M. F. de Godoy, G. Li, B. Macek, P. Mortensen, R. Pesch, A. Makarov, O. Lange, S. Horning, M. Mann, Parts per million mass accuracy on an Orbitrap mass spectrometer via lock mass injection into a C-trap. Mol. Cell. Proteomics MCP. 4, 2010–2021 (2005).

Acknowledgments: We thank Loïc Lepiniec for providing the *tws1-1* and *tws1-2* seeds, Carlos Galvan Ampudia, Yvon Jaillais and Laia Armengot for materials and helpful discussions, Audrey Creff, Ursula Glück-Behrens, Alexis Lacroix, Patrice Bolland, Justin Berger, Isabelle Desbouchages and Hervé Leyral for technical assistance, Angélique Patole, Brigitte Martin Sempore, Cindy Vial and Stéphanie Maurin for administrative assistance and Berit Würtz and Jens Pfannstiel (Core Facility Hohenheim) for mass spectrometric analyses. TEM images were acquired at the Centre Technologique des Microstructures, Université Lyon1.

Funding: The study was financed by joint funding (project Mind the Gap) from the French Agence National de Recherche (ANR- 17-CE20-0027) (G.I.) and the Swiss National Science Foundation (NSF) (N.G., supporting S.F.). N.M.D. was funded by a PhD fellowship from the Ministère de l'Enseignement Supérieur et de la Recherche. Funding was also provided by NSR grant no 31003A_176237 (M.H.) and an International Research Scholar grant from the Howard Hughes Medical Institute (to M.H). S.O. was supported by a long-term postdoctoral fellowship by the Human Frontier Science Program (HFSP). S.R. was supported by a PhD fellowship from the Carl-Zeiss Foundation.

Author contributions: G.I. led the study. G.I. and N.G. obtained funding for the study. G.I., N.G., A.Sc., M.H. T.W and A.St. supervised the work. N.M.D., S.R., S.F., S.O. and S.C. carried out the experiments. All authors were involved in the analysis of the results. G.I., A.Sc. and N.M.D. wrote the paper with input from all authors.

Competing interests: The authors declare no competing interests.

Data and materials availability: All lines used in the study will be provided upon signature of an appropriate Material Transfer Agreement. All data is available in the main text or the supplementary materials.

Supplementary Materials:

Materials and Methods

Figures S1-S23

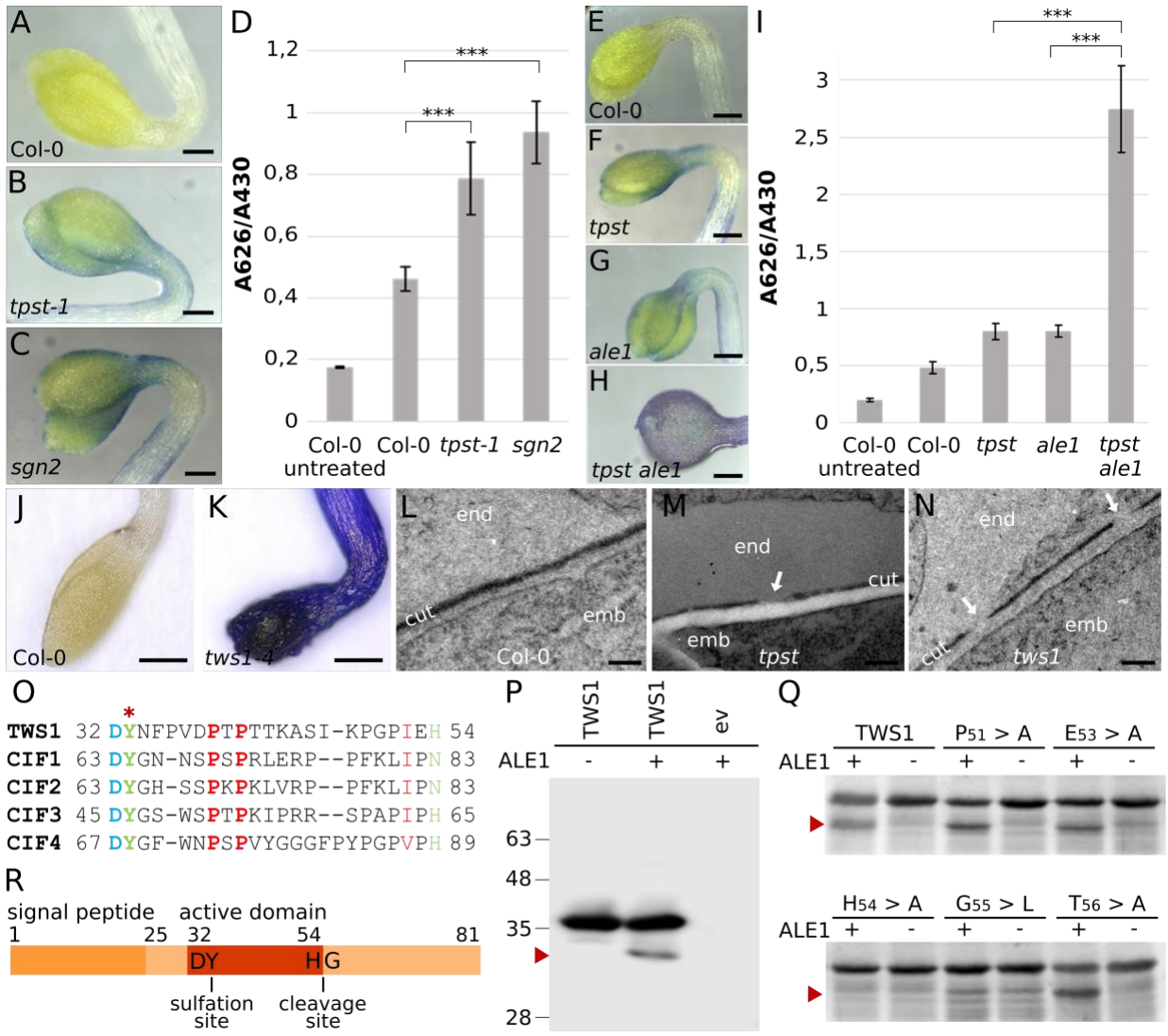

Fig. 1. TPST and ALE1 are required for maturation of the TWS1 peptide. A-C, E-H and J-K) Toluidine blue tests on etiolated cotyledons. Scale bars = 200µm. D and I) Quantification of toluidine blue uptake by the aerial parts of young seedlings, normalized to chlorophyll content. N=6, ten seedlings per repetition. *** = statistical differences with one-way ANOVA followed by a *post-hoc* Scheffé multiple comparison test ($P < 0,01$) in D and I. J and K) Toluidine blue permeability of *tws1-4* compared to Col-0. Scale bars = 400µm L-M) Transmission electron micrographs of the embryo/endosperm interface at the heart stage. Scale bars = 200nm. Genotypes are indicated, and gaps in the cuticle are shown by white arrows. O) The predicted TWS1 active peptide sequence and alignment with four other known GSO ligands (CIF1,CIF2, CIF3 and CIF4). The site of predicted sulfation is indicated with a red asterisk. P) Anti-His western blot of protein extracts from *N. benthamiana* leaves agro-infiltrated to express TWS1::GFP(His)6 (TWS1) or the

empty vector (-). Co-expression of ALE1::(His)6 or the empty-vector control are indicated by + and -, respectively. Q) Coomassie-stained SDS-PAGE showing recombinant GST-TWS1 and the indicated site-directed mutants digested *in vitro* with (+) or without (-) ALE1-(His)6 purified from tobacco leaves. Arrows indicate specific cleavage products. R) The full length TWS1 precursor. Sulfation and ALE1 cleavage sites are indicated.

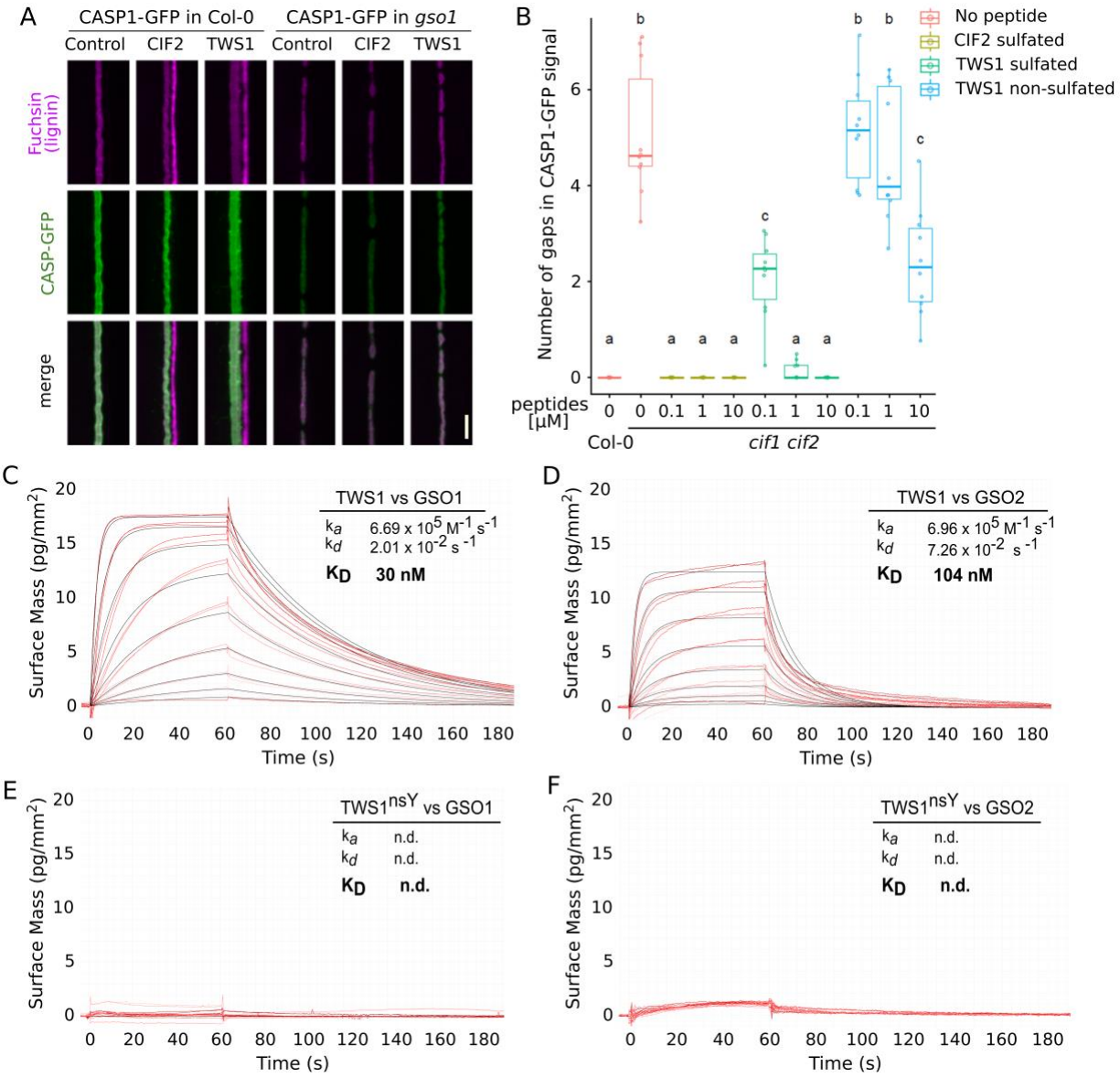

Fig. 2. The TWS1 peptide is a functional GSO1/GSO2 ligand. A) Root over-lignification following treatment with the active CIF2 or TWS peptide in Col-0 and in the *gso1 (sgn3-3)* background. Lignin is stained in purple and CASP-GFP fusion protein, marking the Casparian strip domain, in green. Scale bar = 5µm B) Complementation of *cif1-2 cif2-2* Casparian strip integrity phenotype by peptide treatments. Number of gaps in CASP1-GFP signal counted after treatment with CIF2 sulfated peptide, TWS1 sulfated peptide, TWS1 non-sulfated peptide. N=10. a, b, and c correspond to a classes statistically supported by one-way ANOVA analysis followed by Tukey tests ($P < 0,05$). C-F) Grating-coupled interferometry (GCI)-derived binding kinetics. Shown are sensorgrams with raw data in red and their respective fits in black. k_a, association rate

constant; k_d, dissociation rate constant; K_D, dissociation constant. C) on the GSO1 extra-cellular domain in the presence of the sulfated TWS1 peptide. D) on the GSO2 extra-cellular domain in the presence of the sulfated TWS1 peptide. E) on the GSO1 extra-cellular domain in the presence of the non-sulfated TWS1 peptide. F) on the GSO2 extra-cellular domain in the presence of the non-sulfated TWS1 peptide.

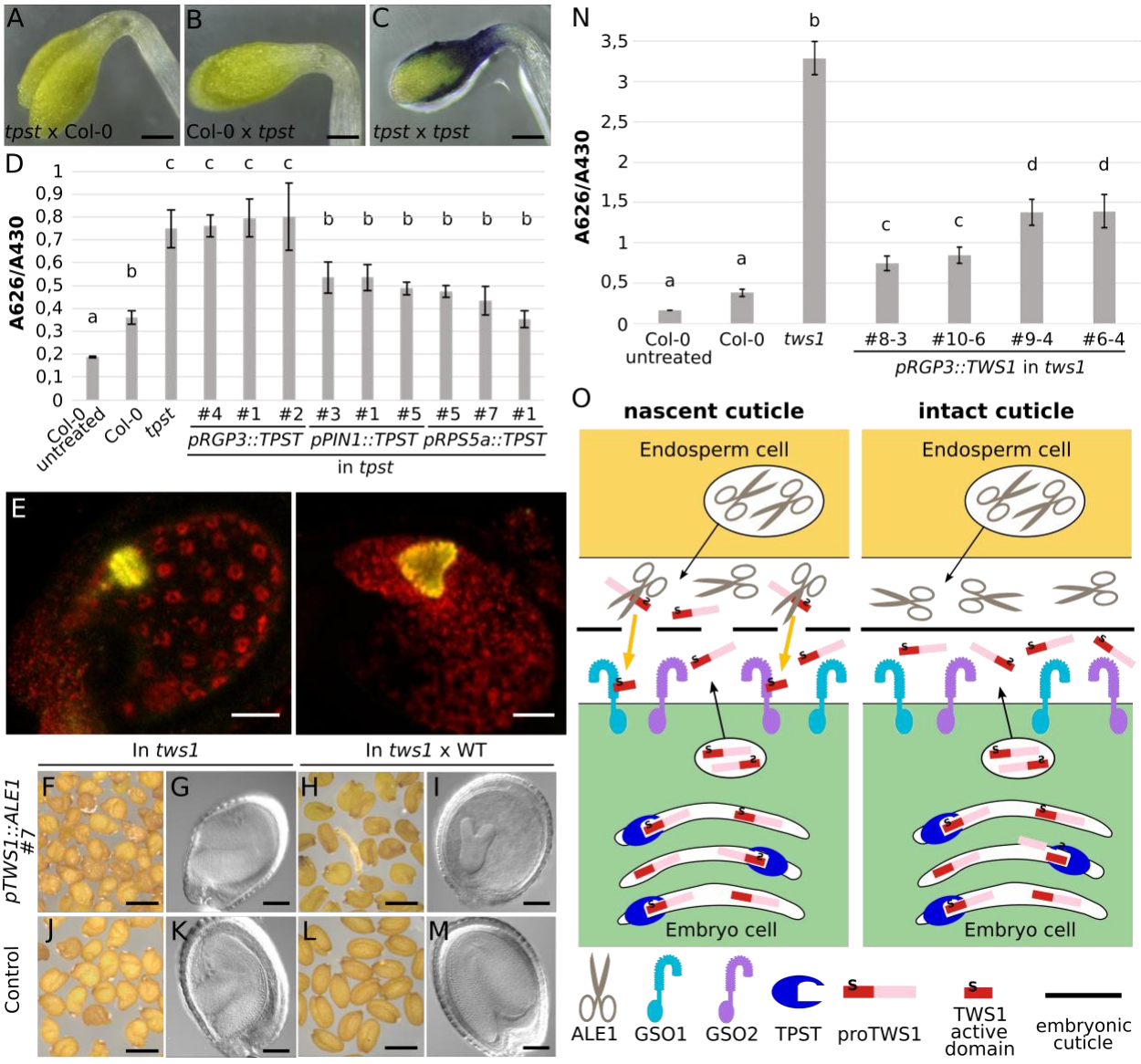

Fig. 3. Spatial separation of *ALE1* and *TWS1* expression is critical for pathway function. A-C) F1 seedlings from reciprocal crosses stained with Toluidine blue. D,N) Toluidine blue quantification as in Fig. 1. a-d = statistical differences with one-way ANOVA followed by a *post-hoc* Scheffé multiple comparison test (P < 0,01). D) Complementation of *tpst-1* mutant with endosperm-specific expression of *TPST* (*pRGP3::TPST*), embryo-specific expression of *TPST (pPIN1:TPST)* and ubiquitous expression of *TPST (pRPS5a::TPST)* compared to *tpst-1* and Col-0. 3 independent lines were analysed. E) Confocal images of *pTWS1::mCitrine::NLS-mCitrine* reporter lines, signal in yellow, autofluorescence in red. Scale bars = 50µm. F,G) Dry seeds (scale

bars = 400 µm) and chloral hydrate cleared seeds (9 DAP) (scale bars = 100 µm) respectively from a line expressing *ALE1* in the embryo in the *tws1-4* background (*pTWS1::ALE1 line#7*). H,I) Seeds from crosses of Col-0 pollen onto *line#7*. J,K) self-fertilized *tws1-4* seeds as a control L,M) Seeds from a cross of Col-0 pollen on a *tws1-4* pistil as a control. Results for three further independent transgenic lines are shown in Figs. S18 and S19. N) Complementation of *tws1-4* mutants by expression of TWS1 in the endosperm. Four independent lines were analysed. O) Model for embryonic cuticle integrity monitoring. Panel on left shows the wild-type situation prior to gap-filling (nascent cuticle), illustrating the diffusion and processing of TWS1 across the embryo-endosperm interface. Panel on right shows the wild-type situation when the cuticle is intact, spatially separating signalling components and thus the attenuating signalling.